AEROELASTIC STABILITY ANALYSIS OF TWO HINGELESS ROTORS

Italo Cafarelli [1], A. Stewart Hopkins[2], Khiem Van Truong [3], Thomas Maier [4]

[1 and 3] ONERA
29 Avenue de la Division Leclerc, 92320 Châtillon, France
e-mail: italo@onera.fr , truong@onera.fr

[2 and 4] Aeroflightdynamics Directorate
US Army Aviation and Missile Research, Development and Engineering Center
Ames Research Center, Moffet Field, CA 94035
e-mail: ahopkins@mail.arc.nasa.gov , tmaier@mail.arc.nasa.gov

Keywords: Hingeless, rotorcraft, aeroelasticity, stability

Abstract. Calculations from three comprehensive rotorcraft computer programs were correlated with experimental data from two hingeless rotors. Results calculated with CAMRAD II, HOST, and RCAS were correlated with regressing lag mode damping data from experiments with two hingeless, soft-inplane rotors, one with straight blades and the other with swept-tip blades. Experimental data was available for hover as well as forward flight. The basic characteristics of and the models used with the computer programs are described. A variety of inflow models were used including uniform, Pitt-Peters and Peters-He type dynamic inflow, and free wake. *In vacuo* fan plots are compared. Correlations of regressing lag mode damping as functions of precone angle, collective angle, and inflow model are presented for both rotors in hover. And, correlations of regressing lag mode damping as functions of shaft angle, precone angle, collective angle, advance ratio, and inflow model are presented for selected configurations for both rotors in forward flight.

NOMENCLATURE

c	Chord 0.08636m (3.4 in)
R	Rotor radius for both rotors: R = 1.143m (3.75 ft)
V	Wind tunnel speed (m/s)
α_S	Shaft angle (positive for forward tilt) (deg.)
β_P	Precone angle (positive tip up) (deg.)
θ_0	Collective pitch (deg.)
μ	Advance ratio: $\mu = V \cos \alpha_S / \Omega_0 R$
σ	Real part of eigenvalues; minus damping (rad/s)
ω_n	Natural frequency of mode (rad/s)
Ω	Rotor speed (rad/s)
Ω_0	Nominal rotor speed =178.0 rad/s (1700 RPM)
ζ	Fraction of critical damping
1x1	Peters-He type dynamic inflow model whose highest power of radial terms is one and whose maximum number of harmonics is one
4x4	Peters-He type dynamic inflow model whose highest power of radial terms is four and whose maximum number of harmonics is four

1. INTRODUCTION

For many years, under the auspices of the US/France Memorandum of Agreement (MoA) for Cooperative Research on Helicopter Aeromechanics, the US Army Aeroflightdynamics Directorate (AFDD) and the French Office National d'Etudes et de Recherches Aérospatiales (ONERA) have jointly pursued selected rotorcraft research topics. Substantial attention has been devoted to the aeroelastic stability of nonarticulated rotors, as part of the first task of the MoA (Rotorcraft Aeroelasticity).

Lead-lag damping is one of the most crucial design parameters for soft-inplane, hingeless rotors. The sensitivity of damping predictions to aerodynamic and dynamic models exposed a need for high quality experimental data, suitable for validating the analyses. The partners undertook the design and test of hingeless (AFDD) and bearingless (ONERA) isolated rotors. AFDD developed two soft-inplane hingeless rotors (sometimes referred to as the Advanced Dynamic Model or ADM) and conducted a series of tests in hover and forward flight. The first rotor (ADMSTR in the figures) had straight blades [1, 2], while the second (ADMSWP in the figures) had swept-tip blades [3].

Over the years, several papers reported the correlation of experimental results with those obtained with various computer programs. Initial correlation efforts, for each rotor, were carried out with CAMRAD/JA and CAMRAD II [1, 3]. A subsequent sensitivity study that led to an improved model also used CAMRAD II [4]. Correlation using dynamic stall and dynamic wake models are reported in [2]. Both partners developed in-house comprehensive analysis programs. (Eurocopter and ONERA developed HOST and AFDD developed RCAS.) Attention then turned to correlation with those codes [5]. This paper presents the latest *in vacuo* comparisons and the latest hover and forward flight correlations that have been obtained with the CAMRAD II, HOST, and RCAS computer programs. Particular attention is paid to ways in which changes in the aerodynamic model affect the correlation.

2. DESCRIPTION OF THE EXPERIMENTS

Reference [1] offers a thorough description of the first model rotor, which had straight blades, and of the hover chamber and wind tunnel tests that were conducted. Similarly, reference [3] describes the second model rotor, which had swept-tip blades and the tests that were conducted with it. Some of the most important characteristics of those models and tests are summarized here.

2.1 Description of the experimental models

Both tested models were R = 1.143m radius, Mach scaled, hingeless rotors consisting of a nearly rigid hub and four blades, each with a 0.08636m chord and a NACA 0012 airfoil section. To emphasize the effects of pitch-lag coupling, the flexure and constant regions of the blades were designed with relatively low torsional stiffness. Although the blades were designed to have no twist, the straight blades had small, but significant, twist irregularities, which varied both spanwise and from blade to blade. The experimenters adjusted each blade's root pitch to track the blade tips. They measured the root pitch differences to provide and average rotor collective pitch. The pitch angle was adjusted so that the average pitch at 0.75R matched the commanded pitch, $\theta(0.75R) = \theta_0$.

The straight and swept-tip blades are shown in Fig. 1, which also identifies the four (straight) or five (swept-tip) regions that constituted the blades:

1) The first, rigid-hub, region was very stiff and consisted of a portion of the hub, the feathering bearing, and the blade attachment hardware.
2) The second, flexure, region had enough flexibility to allow substitution of elastic deformation for the classical flap and lag articulations (similar to the BO-105 hingeless rotor).
3) The third, transition, region was a short relatively stiff transition between the flexure and airfoil sections. There is some uncertainty regarding the spanwise variation of mechanical properties for this region. There was a single weight measurement and the rapidly changing elastic properties were not measured.
4) The fourth, constant, region had a NACA 0012 airfoil section and nearly coincident quarter chord, control axis, mass center, elastic axis, tensile axis, and aerodynamic center. Properties for this region were carefully measured.
5) The fifth, swept-tip region (swept-tip blades only) sheared the section outboard of 0.9R 30^{o} aft. To keep the center of mass near the quarter chord a substantial balance mass was located near 0.9R and the leading edge.

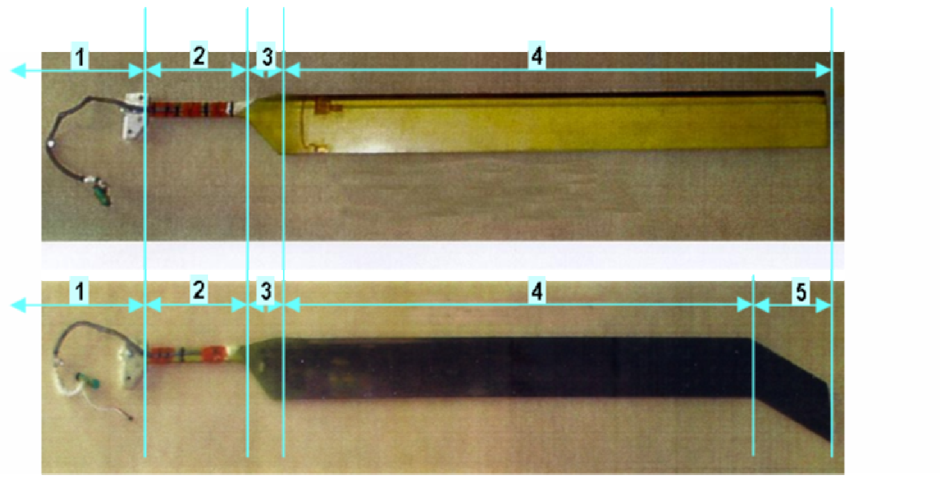

Figure 1: Region identification for straight and swept-tip blades

2.2 Description of the tests

Hover data were obtained in the AFDD Anechoic Hover Test Chamber, as follows:
1) The shaft angle was fixed at $\alpha_S = 0^o$.
2) Hub precone angles were set at either $\beta_P = 0^o$ or 2^o.
3) A rotor speed, Ω, was selected. (Only nominal rotor speed, Ω_0 =178.0 rad/s, results are reported in the present paper).
4) A collective pitch in the range $-11^o \leq \theta_0 \leq 11^o$ was selected.
5) Transients were allowed to die out before starting the damping measurement procedure.

Forward flight data were obtained in the Army/NASA 7-By 10-Foot Wind Tunnel at Ames Research Center. Figure 2 shows the two rotors installed in the tunnel on the Rotor Test Rig. The fixed system rotor balance of the test stand was locked out to minimize coupling of rotor and stand dynamics. As a result, no direct thrust or hub moment data were available. However, the flap moments, measured at 0.12R, have been used to estimate them. Potentially less accurate, low advance ratio ($\mu < 0.1$), experimental results were not reported in [3,4], but have been included here. Only a few representative subsets of the configurations tested have been selected for comparison in the present paper.

Figure 2: Straight and swept-tip models in Army/NASA 7-By 10-Foot Wind Tunnel

Forward flight data were obtained as follows:

1) Hub precone angles were set at either $\beta_P = 0^o$ or 2^o.
2) The shaft angle was fixed at $\alpha_S = 0^o$, 3^o, or 6^o. (This positive-tilt-forward sign convention is the opposite of that used in [1-5].)
3) A rotor speed, Ω, was selected (only results for Ω_0 are reported in the present paper).
4) An integral collective pitch angle, in the range $0^o \leq \theta_0 \leq 7^o$, was selected. (However, after adjusting for twist irregularities in straight blades the effective collective angles were off by a few tenths of a degree.)
5) Wind tunnel airspeed was increased to obtain the desired advance ratio $0 \leq \mu \leq 0.51$.
6) The rotor was brought into trim by adjusting the cyclic pitch; so the 1/rev flapping moment (as measured by the bending moment at 0.12R) was minimized.
7) The rotor was allowed to reach periodic equilibrium, before making a measurement.

2.3 Regressing lag mode damping measurement

The basic measurement approach was to excite the regressing lag mode and infer its damping from the rate of decay. Low amplitude cyclic excitation was applied at the (fixed frame) regressing lag mode frequency (using one of the stand's higher harmonic control actuators). The frequency was adjusted to maximize the lead/lag response and the amplitude was adjusted to near the structural limit. Excitation was turned off and data were acquired. For the rotor with straight blades, a multi-blade coordinate transform was used to convert the moments obtained from the gauges to (fixed frame) regressing lag moments. For the rotor with swept-tips, due to issues with blade #1, the (rotating frame) blade #3 lag moments were used. A moving-block analysis was applied to the moment, and the decay of the signal amplitude at the lag mode frequency was used to infer the damping. The reported damping values are the negative of the real part of the dimensional eigenvalues ($-\sigma$).

2.4 Basic characteristics of the experiment

There are certain general behaviors that would have been expected of the rotors during test. Described in more detail below, these included: 1) Reduced effective collective resulting from a swept tip, 2) Damping symmetry with respect to collective, 3) Shift of effective collective resulting from precone, 4) Damping increases with the magnitude of the collective, and 5) Damping reductions that grow with advance ratio, resulting from shaft angle.

For the swept-tip blade, the lift on the tip was aft of the control axis, which resulted in a torsional moment on the blade. A moment also results from inertial effects associated with the swept tip's large torsional moment of inertia (arising from the combination of the balance mass forward and the swept-tip mass aft). Torsional flexibility resulted in significant twist in the flexure and constant regions of the blade (on the order of $\theta_0/2$) in a direction opposite the commanded pitch, θ_0. The behavior of a swept-tip blade at a collective θ_0 is approximately like that of a straight blade at collective $\theta_0/2$.

For a fully isolated rotor with symmetric blade profiles and $\beta_P = 0^o$ precone, the regressing lag mode damping should be symmetric about $\theta_0 = 0^o$. Small, but significant asymmetry was observed in the experimental data. Twist irregularities accounted for some of the asymmetry for the rotors with straight blades. However, asymmetry was also apparent with swept-tip blades (and in other tests). The reasons for this asymmetry have not been fully explained.

When the precone was set to $\beta_P = 2^o$, there was some small positive collective such that the coning from thrust approximated the precone. As a result, the flap deformation was minimal, which in turn minimized pitch-lag coupling and consequently damping. Thus an apparent effect of precone was to shift the damping as a function of collective curve to the right, along the collective axis.

As the magnitude of the collective (relative to the minimal flap deformation value, if there was precone) increased, the flap bending increased, introducing pitch-lag coupling, which lead to larger damping. Thus, larger collectives (and thrust) lead to larger damping.

As the shaft angle was increased, a portion of the tunnel velocity ($V \sin \alpha_S$) was directed down through the rotor, which reduced blade angle of attack and thrust. Consequently, the damping dropped as the shaft angle was increased. Furthermore, as advance ratio increased, the magnitude of the drop in damping grew.

The qualitative patterns in the experimental data from the experiment confirmed all of these expectations.

3. COMPUTER PROGRAM COMPARISON

Three, roughly equivalent comprehensive computer programs for rotorcraft analysis were used to analytically simulate the experiment, CAMRAD II, HOST, and RCAS.

3.1 CAMRAD II overview

CAMRAD II (Comprehensive Analytical Model of Rotorcraft Aerodynamics and Dynamics) is an aeromechanical analysis of a helicopter or rotorcraft that incorporates a combination of advanced technology, including multibody dynamics, nonlinear finite elements, structural dynamics, and rotorcraft aerodynamics. It calculates performance, loads, vibration, response, and stability applicable to a wide range of problems, and a wide class of rotorcraft. Reference [6] describes some of the development background for CAMRAD II. Detailed descriptions of the capabilities and theoretical background are available in a collection of manuals [7].

3.2 HOST overview

HOST (Helicopter Overall Simulation Tool) is a comprehensive tool, developed by Eurocopter [8], which enables the study of helicopter aeromechanics, including handling qualities, static and dynamic loads calculations, rotor design, performance predictions, stability analyses, and flight simulations. It has a very flexible organization and offers several levels of models, ranging from very simple analytical ones to more sophisticated ones (e.g., elastic blade or rotor wake). Several inflow models are currently available in HOST: 1) Steady inflow models including Coleman and Glauert or Meijer Drees, 2) First harmonic inflow models (i.e., Pitt & Peters), 3) Generalized dynamic inflow models (Peters-He based Finite State Unsteady Wake: FiSUW [9]), and 4) Wake models (prescribed METAR or free wake MESIR). A specific model simulates each component of the helicopter. The full configuration is defined by a set of data and managed by HOST kernel.

3.3 RCAS overview

RCAS (Rotorcraft Comprehensive Analysis System) is a comprehensive multi-disciplinary, computer software system for predicting the performance, stability and control, aeroelastic stability, loads and vibration, and aerodynamics characteristics of rotorcraft. Reference [10] provides an overview of RCAS' development history, design, and capabilities, as well as the results obtained for selected problems. The RCAS User's Manual [11] and the RCAS Theory Manual [12] provide more detailed descriptions of RCAS' capabilities and basis. An important feature in RCAS is the association of a different reference frame with each element, allowing large rigid body motions as well as deformation. The resulting accuracy, for a number of well defined laboratory experiments and known analytical solutions, was investigated in a recent article [13].

4. MODELS

Although generally similar, the models developed for each of the computer programs did vary in some details. For each of the three programs, the models developed for this analysis are described below.

The twist irregularities in the straight blades were handled in the same manner for all three programs. The blade to blade dissimilariities in the straight blades, which arose from twist irregularities, were ignored and the average of the irregular twist distributions was used for all of the blades. (Due to blade changes, different average twist distributions were used for hover and for forward flight.)

4.1 CAMRAD II model

The CAMRAD II models are unique in that no new results have been calculated; rather, results generated in the extensive studies reported in [4] or, in a few cases, [3] are presented again. Some of the more important characteristics of the model were:

1) Three beam elements were used to represent the flexure and four elements were used for the remainder of the blade.
2) Twelve rotating blade modes were used and modal damping values of $\zeta = 0.38\%$ and $\zeta = 0.32\%$ of critical damping were used for the straight and swept-tip blades respectively.
3) Fifteen aerodynamic segments and a NACA 0012 2-D table were used to represent the airfoil.
4) The baseline hover calculation used uniform inflow, a hover inflow correction factor = 1.1, tip loss factor = 0.98, and a momentum theory dynamic inflow model.

5) Forward flight calculations were made by suppressing the Pitt-Peters dynamic inflow model and using a free wake to calculate inflow and deformation. Trim was achieved by setting the cyclic to obtain zero pitch and roll moments.
6) Eigenanalysis was performed using Floquet-Lyaponov theory and multiblade coordinates with Pitt-Peters dynamic inflow enabled.

The term "new" model refers to the improved model described in [4]. The term "old" model refers to the baseline model described in [4], which is the same as the model described in [3]. The "old" model differed from the "new" models in that:

1) The flexure was modeled with two beam elements instead of three.
2) Pitt-Peters dynamic inflow and free wake analysis were both used for forward flight.

4.2 HOST model

The rotors were modeled with four identical blades. Each straight blade was modeled with fourteen beam elements (one for the root, three for the flexure, two for the transition, and eight for the constant region). Each swept-tip blade was modeled with eleven elements (one for the root, one for the flexure, two for the transition, six for the constant region, and one for the swept-tip). The concentrated balance weight was distributed in the last element of the constant region, which was extremely short (0.003m). Gravitational effects were included. The elastic blade model was converted to a modal representation retaining the first eight modes. Structural modal damping values of $\zeta = 0.45\%$ and $\zeta = 0.43\%$ of critical were used for the straight and swept-tip blades respectively. These values were derived from the $\beta_P = 0^o$ hover experimental results by fitting second to fourth order polynomials and selecting the value that made the HOST result match the polynomial at $\theta_0 = 0^o$.

The aerodynamic model used thirty segments for the straight blades and twenty-three segments for the swept-tip blade. NACA 0012 2-D airfoil tables were used. Yawed flow and Theodorsen unsteady aerodynamics for moment and lift coefficients were taken into account. Inflow models included uniform, Pitt-Peters, 1x1 and 4x4 dynamic inflow. Tip loss was only modeled in the straight blade computations with the Pitt-Peters dynamic inflow. Calculations were based on an altitude of 1174m.

The analysis procedure started with trim, minimizing the pitch and roll hub moments (4 N·m maximum for both rotors). Once trim was obtained, it was perturbed to obtain the corresponding linear system, which consisted of the mean and first cyclic components for each modal displacement and velocity. Constant coefficient eigenanalysis was then applied to the mean component of the linearized system.

4.3 RCAS model

The two experimental rotors were each modeled in RCAS as a four-bladed rotor, rotating at the prescribed speed, and oriented at the prescribed shaft angle, relative to an inertial frame. Gravitational effects, although not very significant, were included The blades were mounted to the hub at the prescribed precone angle. The assembly was rigid inboard of the pitch bearings, which rotated the blades by the commanded pitch. Each model had four identical blades. Each blade was modeled as seventeen nonlinear beam elements. A rigid body mass element representing the concentrated balance weight near 0.9 R was added for swept-tip blades.

The aerodynamic model used eighteen aerodynamic segments. For the swept tip, the five aerodynamic segments were staggered, each with its leading edge parallel to the unswept portion of the blade (rather than parallel to the swept leading edge of the tip). The airfoil properties were interpolated from standard NACA 0012 2-D airfoil tables. Corrections for yawed flow were not made. Unsteady flow effects were reflected using an approximation to Greenberg-Theodorsen theory. No dynamic stall effects (e.g., Leishmann-Beddoes or ONERA) were used. For each inflow model, some results were calculated with no tip loss, while others were calculated with lift suppressed outboard of 0.98 R Atmospheric properties were for standard conditions at sea level. Results were calculated for three inflow models: 1) uniform momentum inflow, 2) Peters-He dynamic inflow whose highest power of radial terms is one and whose maximum number of harmonics is one, abbreviated 1x1 (essentially Pitt-Peters dynamic inflow) or 3) Peters-He dynamic inflow whose highest power of radial terms is four and whose maximum number of harmonics is four, abbreviated 4x4.

Blade modes were calculated and a modal reduction procedure retained degrees of freedom corresponding to the first eight modes. Modal damping values of $\zeta = 0.38\%$ and $\zeta = 0.32\%$ of critical damping were used for the straight and swept-tip blades respectively. A multi-blade coordinate transform was applied to the equations, associating the calculations with the fixed frame. Periodic equilibrium was obtained by integrating the equations (using seventy-two steps per revolution) until the structural displacements and velocities for successive revolutions were within 0.0003 m and 0.3 m/sec. Trim was obtained by adjusting the cyclic pitch controls until the hub moments were less than 0.27 N·m. The trimmed periodic equilibrium equations were numerically linearized at each azimuth. No Floquet analysis was performed. Instead, the coefficient matrices for the seventy-two azimuths were averaged, and the constant coefficient approximation eigensolutions are reported here. Some of these results have been reported previously [5]. The current results differ from the previous due to improvements in the model, trim convergence, and constant coefficient approximation calculations.

4.4 Model Differences

Although the three models were generally similar, there were some differences that may have affected correlation:

1) As noted in [4], CAMRAD II results were sensitive to the number of beam elements used to represent the flexure region. Significant discrepancies were associated with using less than three elements. This may have affected "old" CAMRAD II and swept-tip HOST results.
2) The use of different values for structural damping, ζ, biased the damping ($-\sigma = \omega_n \zeta$) calculated with HOST relative to that calculated with CAMRAD II or RCAS. For straight blades, the 0.07% difference in ζ resulted in HOST damping values 0.064 greater than those in CAMRAD II or RCAS (which was not too significant compared to typical damping values of 1.0 to 2.0). However, for swept-tip blades, the 0.11% difference in ζ resulted in HOST damping values 0.123 greater than those in CAMRAD II or RCAS (which is significant compared to typical damping values of 0.5 to 1.5).
3) The CAMRAD II analysis method (free wake without Pitt-Peters dynamic inflow for equilibrium and with Pitt-Peters inflow for eigenanalysis) differed significantly from the HOST and RCAS analysis methods (Peters-He 4x4 dynamic inflow for equlibrium and eigenanalysis). Similar differences were shown to significantly affect damping in [4].
4) As noted in [3], there were significant differences between the Floquet eigenvalues (used for CAMRAD II results) and the less accurate constant coefficient approximation eigenvalues (used for HOST and RCAS results).

5. *IN VACUO* COMPARISONS

Figure 3 presents fan plots (normalized blade natural frequencies, ω_n/Ω_0 *vs.* normalized rotor speed, Ω/Ω_0) for straight and swept-tip blades with $\beta_P = 0^o$ precone and $\theta_0 = 0^o$ collective pitch. The presence of the swept-tip introduced coupling between the torsion and flap degrees of freedom not present in the straight blade. Consequently, for straight blades, the first torsion (the third mode at nominal rotor speed) and the second flap (fourth mode) crossed, without coupling, at a rotor speed of about 0.8 Ω/Ω_0. For swept-tip blades, the modes were highly coupled and never crossed. Furthermore, the modes changed character with increasing rotor speed. The third mode started as second flap and took on the character of first torsion at high rotor speeds while the fourth mode started as first torsion and became second flap.

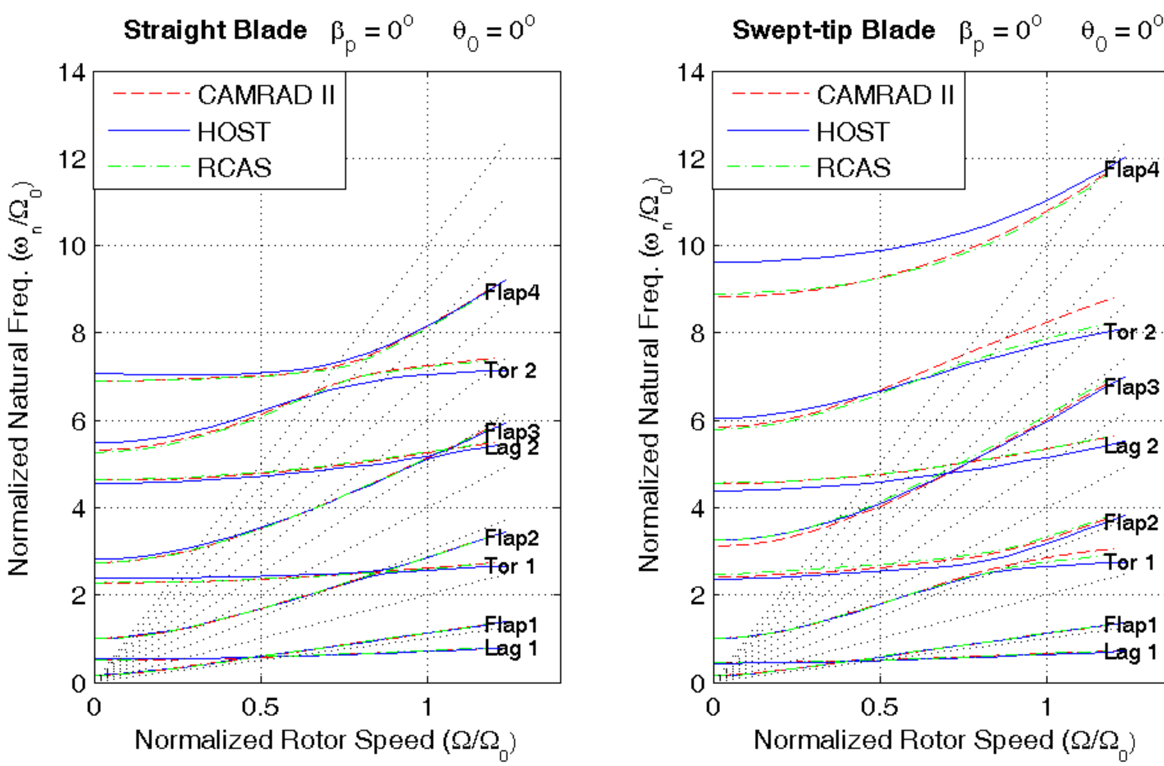

Figure 3: Fan plots for straight and swept-tip rotating blades

No *in vacuo* rotating blade frequencies were measured, so comparisons could only be made between the three computer programs. Although all of the codes captured the behavior of the modes, numerical agreement was better for lower frequency modes and for straight blades. The first lag, first flap, and first torsion frequencies (at $\Omega/\Omega_0 = 1$) were, respectively, within 0.8%, 0.3%, and 2.8% of each other for straight blades, and within 1.5%, 0.44%, and 10% of each other for swept-tip blades. Some discrepancies increased with rotor speed. For instance, at $\Omega/\Omega_0 = 1.2$, the first torsion frequencies were only within 5.7% for straight and 16% for swept-tip blades. The highest frequency modes (e.g., second torsion and fourth flap), showed significant discrepancies at $\Omega = 0$. Model or computer program discrepancies which affected the higher modes were not expected to have much impact on the first regressing lag mode. However, the model discrepancies that led to a 10% difference in the first torsion mode may have affected other comparisons.

6. HOVER COMPARISONS

Experimental hover data were compared with results calculated with the three computer programs (which used a variety of inflow models). Uniform inflow results were obtained for all cases, however some used a tip loss factor of 0.98 and others had no tip loss. The Pitt-Peters dynamic inflow model would be expected to have produced results very similar to the Peters-He 1x1 dynamic inflow model.

All of the CAMRAD II precone $\beta_P = 0^o$ results were generated with the "new" model, while all of the CAMRAD II precone $\beta_P = 2^o$ results were generated with the "old" model. The "old" results for $\beta_P = 0^o$ precone were compared with the "new" results. The "new" and "old" results for straight and swept-tip blades and for uniform and momentum theory dynamic inflow were nearly identical, with the exception of uniform inflow for swept-tip blades (which had large unexplained differences).

6.1 Straight blade hover comparisons

For precone angles, $\beta_P = 0^o$ and 2^o, and the three computer programs, Fig. 4 compares experimental and a variety of computed values (associated with a variety of inflow models) for regressing lag mode damping, $-\sigma$, as a function of collective, θ_0. The following observations can be made:

1) All of the codes captured the basic characteristics of the experiment, discussed previously, including symmetry and the effects of collective and precone.
2) Some asymmetry was evident in the experimental data, with higher damping for negative collectives.
3) Lower damping values were calculated for models with more refined inflow models.
4) Lower damping values were calculated for RCAS models that included tip loss.
5) No major improvement of the correlations can be seen when refining inflow models.
6) HOST models were less sensitive to inflow model refinement than the other programs.

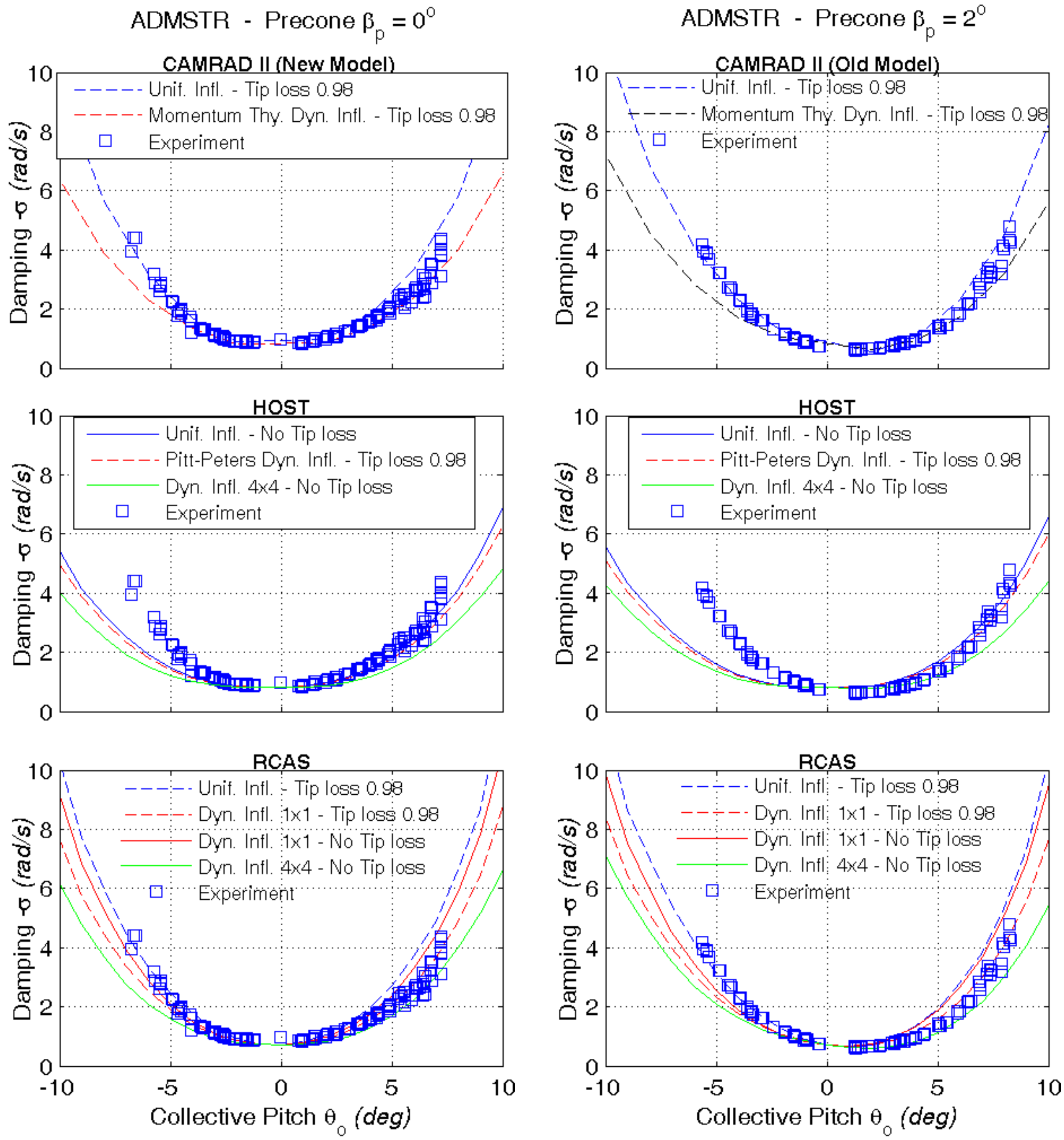

Figure 4: Comparisons for rotors with straight blades in hover

6.2 Swept-tip blade hover comparisons

For precone angles, $\beta_P = 0^o$ and 2^o, and the three computer programs, Fig. 5 compares experimental and a variety of computed values (associated with a variety of inflow models) for regressing lag mode damping, $-\sigma$, as a function of collective, θ_0. The following observations can be made:

1) All of the codes captured the basic characteristics of the experiment, discussed previously, including symmetry and the effects of a swept tip, collective, and precone.
2) The experimental data were much more symmetric than the data for straight blades. Furthermore the asymmetry was in the opposite direction, with higher damping for positive collectives.

3) There were no clear trends in damping values associated with more refined inflow models.
4) In RCAS, including tip loss resulted in higher damping values, the opposite of the behavior for straight blades. All of the models without tip loss agreed well with each other and experiment. However, all of the models with tip loss calculated damping values substantially higher than experiment.
5) HOST models were less sensitive to collective than the other programs or experiment. If the same structural damping as the other programs had been used, most of the experimental values would fall above the calculated results.

.

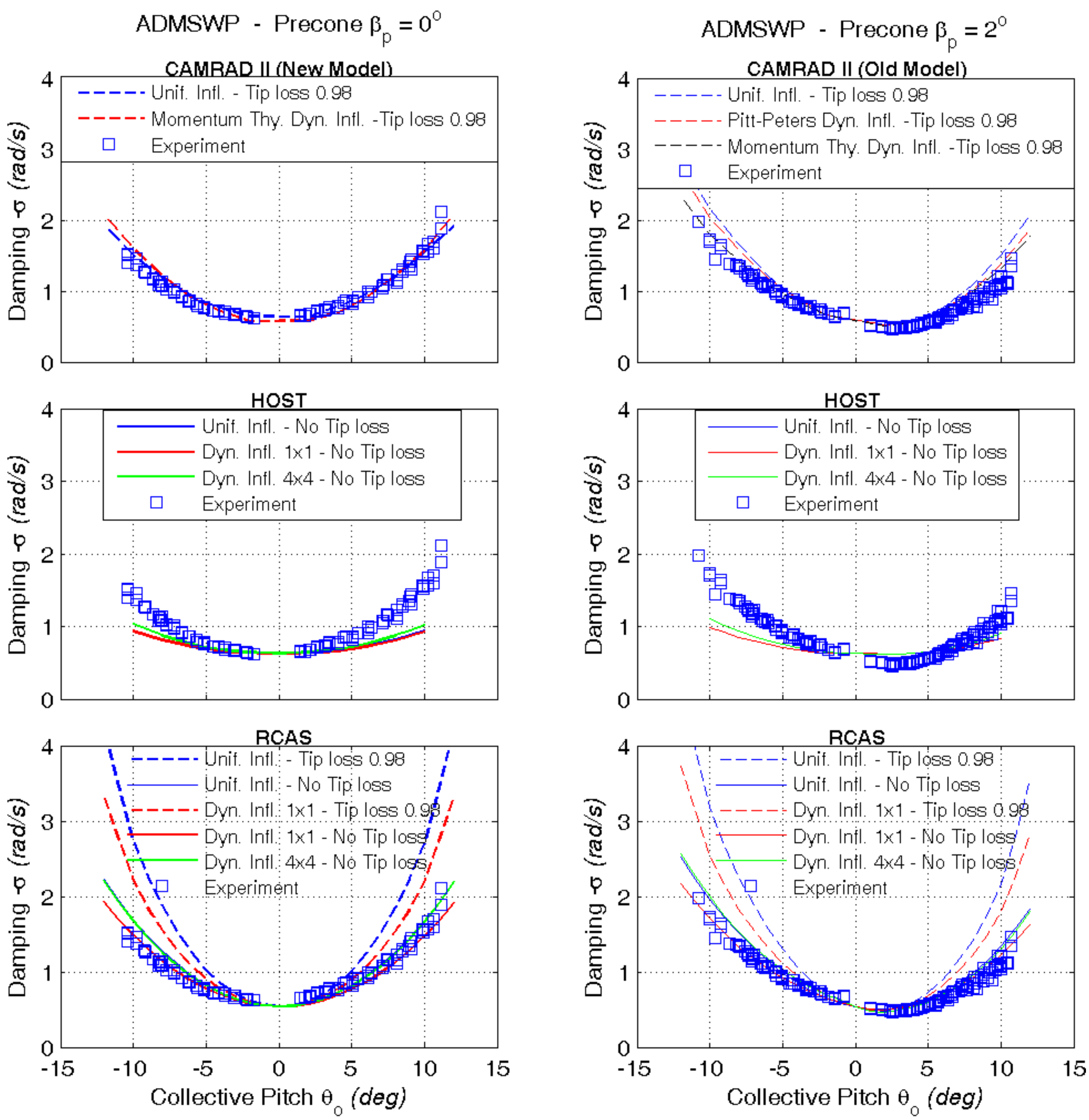

Figure 5: Comparisons for rotors with swept-tip blades in hover

The reversal of the way in which tip loss affected damping is consistent with the previously discussed basic characteristics of the experiment. Suppression of the outboard part of the lift, on the swept tip, reduced the moment and, consequently, the twist in the torsionally soft flexure. The twist did not reduce the commanded pitch as much, so the effective pitch, thrust, and damping were increased. The better agreement between experiment and models without tip loss suggests that the tip loss approximation may have been an inappropriate oversimplification of the flow on the swept-tip.

As noted in the previous discussion of model differences, the sensitivity to model discretization may explain why the correlation was better with the HOST straight blade model than with the swept-tip blade model.

7. FORWARD FLIGHT COMPARISONS

Experimental forward flight data were compared with results calculated with the three computer programs (which used a variety of inflow models). (All CAMRAD II results were calculated with the "new" model.) Uniform inflow results were obtained for many cases, however some used a tip loss factor of 0.98 and others had no tip loss. The Pitt-Peters dynamic inflow model would be expected to have produced results very similar to the Peters-He 1x1 dynamic inflow model, although, again, tip loss was modeled for some cases and not for others. The CAMRAD II free wake model suppressed Pitt-Peters inflow for equilibrium but included it for eigenanalysis.

The correlation information for each blade type has been gathered into two figures. In the first, the collective is fixed and there is a family of curves associated with the three shaft angles. In the second, the shaft angle is fixed and there is a family of curves associated with three collectives. The shaft angle or collective configuration variable is represented by color. Line type is used to differentiate inflow models. Finally, the presence of plus sign markers on a curve signifies a tip loss factor of 0.98. Diamond markers are used to identify one straight blade model which used quasi-steady section aerodynamics for comparison with the usual unsteady aerodynamics.

7.1 Straight blade forward flight comparisons

For a $\theta_0 = 3^o$ collective angle, for $\beta_P = 0^o$ and 2^o precone angles, and for the three computer programs, Fig. 6 compares experimental and a variety of computed regressing lag mode damping values, $-\sigma$, as a function of advance ratio, μ (for $\alpha_S = 0^o$, 3^o, or 6^o shaft angles and a variety of inflow models). For an $\alpha_S = 0^o$ shaft angle with a $\beta_P = 0^o$ precone angle, for an $\alpha_S = 6^o$ shaft angle with a $\beta_P = 2^o$ precone angle, and for the three computer programs, Fig. 7 compares experimental and a variety of computed regressing lag mode damping values, $-\sigma$, as a function of advance ratio, μ (for $\theta_0 = 1^o$, 3^o, or 6^o collective angles and a variety of inflow models). Color is used to distinguish shaft angles in Fig. 6, but it is used to distinguish collective angles in Fig. 7. Unfortunately, no CAMRAD II results were available for the $\beta_P = 0^o$ precone cases.

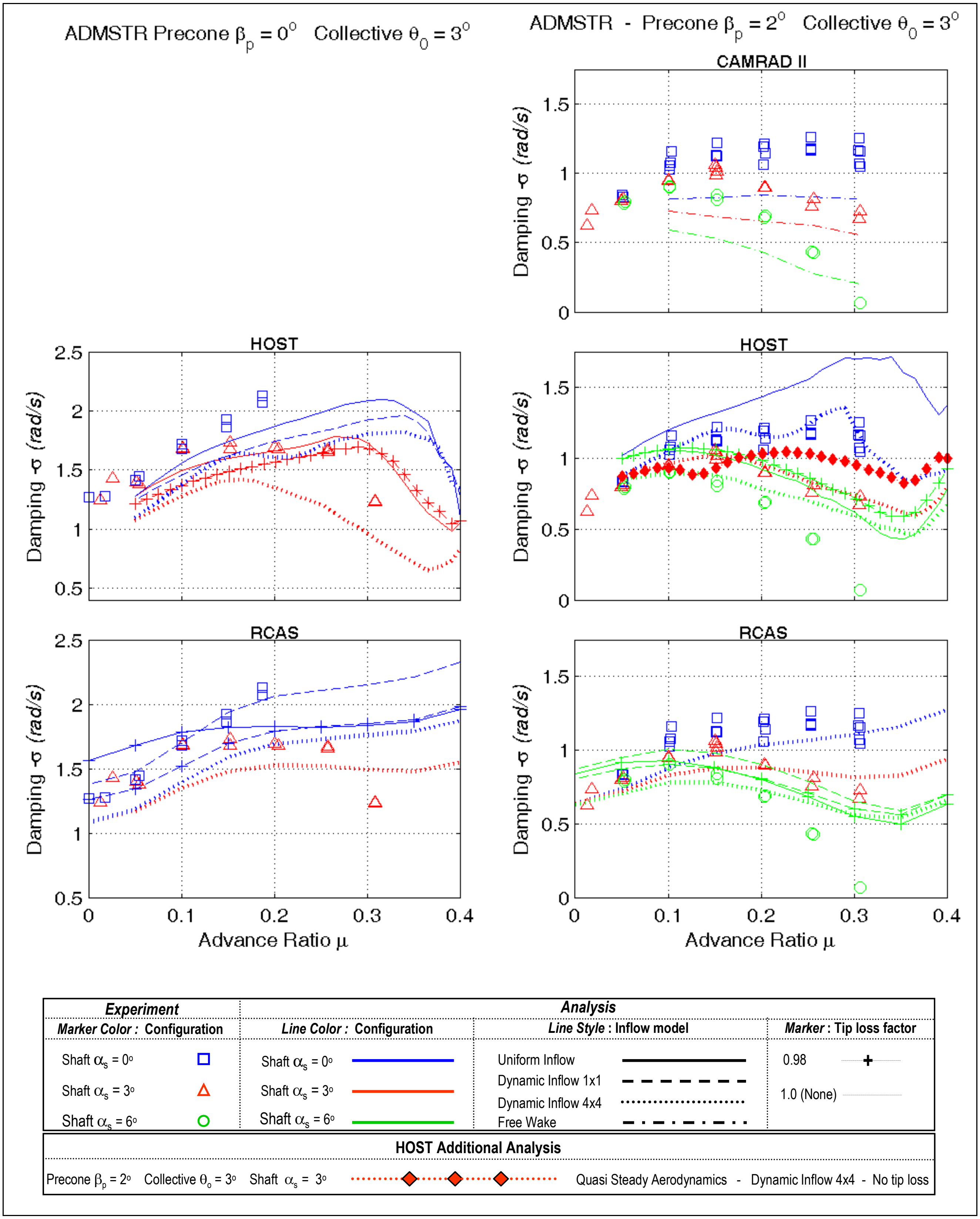

Figure 6: Comparisons for rotors with straight blades in forward flight with shaft angle variations

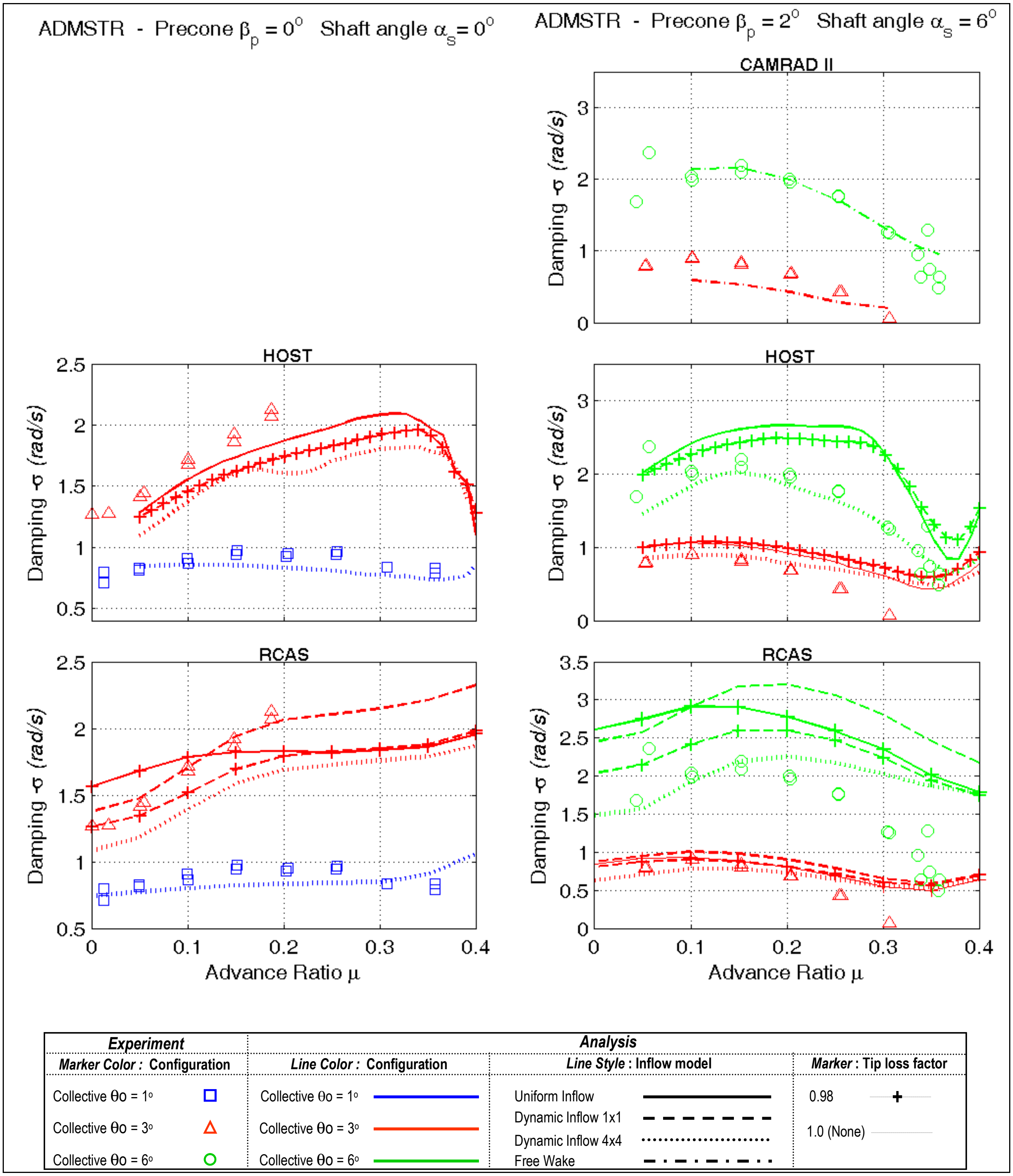

Figure 7: Comparisons for rotors with straight blades in forward flight with collective variations

The following observations can be made:

1) All of the codes captured the basic characteristics of the experiment, discussed previously, including the effects of collective, precone, and the combination of shaft angle and advance ratio.
2) At lower advance ratios, the experimental damping tended to increase with advance ratio, with steeper slopes associated with higher collectives. At higher advance ratios,

with $\alpha_S = 0^o$ shaft angle, the upward slope continued or flattened. However, for higher shaft angles, the damping leveled and then decreased with increasing advance ratio.

3) The computer programs reflected the damping as a function of advance ratio and shaft angle behavior qualitatively, but the quantitative performance was uneven. For instance, when $\beta_P = 2^o$, $\theta_0 = 3^o$, $\alpha_S = 6^o$, and $0.2 \leq \mu \leq 0.3$ the rate of change of the damping with respect to advance ratio was at least double that calculated with any of the computer programs.
4) Lower damping values were calculated for models with more refined inflow models, which was consistent with the behavior of this blade in hover.
5) More refined dynamic inflow models showed better correlation with the data for $\beta_P = 2^o$ but worse correlation with the data for $\beta_P = 0^o$.
6) It appears there was a stability boundary near $\alpha_S = 6^o$, $\beta_P = 2^o$, $\theta_0 = 3^o$, and $\mu = 0.31$. This exceptionally low damping measurement was missed by all of the programs.
7) The importance of the unsteady aerodynamics is illustrated by comparing the $\beta_P = 2^o$, 4x4 dynamic inflow model (FisuW 4x4), HOST results for quasi-steady aerodynamics with those for unsteady dynamics. The unsteady aerodynamics model clearly captured the qualitative and quantitative trends more accurately.

7.2 Swept-tip blade forward flight comparisons

For a $\theta_0 = 3^o$ collective angle, for $\beta_P = 0^o$ and 2^o precone angles, and for the three computer programs, Fig. 8 compares experimental and a variety of computed regressing lag mode damping values, $-\sigma$, as a function of advance ratio, μ (for $\alpha_S = 0^o$, 3^o, or 6^o shaft angles and a variety of inflow models). For an $\alpha_S = 0^o$ shaft angle, for $\beta_P = 0^o$ and 2^o precone angles, and for the three computer programs, Fig. 9 compares experimental and a variety of computed regressing lag mode damping values, $-\sigma$, as a function of advance ratio, μ (for $\theta_0 = 3^o$, 6^o, or 7^o collective angles and a variety of inflow models). Color is used to distinguish shaft angles in Fig. 8, but it is used to distinguish collective angles in Fig. 9.

The following observations can be made:

1) All of the codes captured the basic characteristics of the experiment, discussed previously, including the effects of collective, precone, and the combination of shaft angle and advance ratio.
2) The experimental results consistently showed an increase in damping at the higher advance ratios. All of the codes reflected the same behavior qualitatively, however the magnitude of the increase was way too large for HOST and RCAS but too small for CAMRAD II.
3) There was much less sensitivity to shaft angle than was evident for straight blades. The basic characteristics were still evident in the experimental data and in the results calculated by CAMRAD II and RCAS.
4) The experimental damping, as a function of advance ratio, exhibited a sinuous behavior, with the damping first increasing, then decreasing, and finally increasing again with increasing advance ratio. This “up-down-up” pattern was most apparent for $\beta_P = 0^o$ precone with larger collectives. This behavior was not captured by CAMRAD II or RCAS. HOST exhibited the behavior to a very slight degree with the 4x4 dynamic inflow model. Interestingly, the behavior disappeared with the 1x1 dynamic inflow model which otherwise produced very similar results. However there was no quantitative agreement.
5) There were no clear trends in damping values associated with increasing inflow model refinement. HOST results were very insensitive to inflow model refinement.

6) The effects of tip loss were consistent with the previously discussed effects in hover. The damping values for inflow models with tip loss were significantly higher than for those without. Furthermore, the no tip loss results for different inflow models were relatively close to each other and the experimental data.
7) For low to moderate advance ratios, both CAMRAD II and RCAS results exhibited an increase in damping with increasing advance ratio, a behavior that is not supported by the data.
8) HOST models were less sensitive to collective than the other programs or experiment, which is consistent with the behavior in hover.

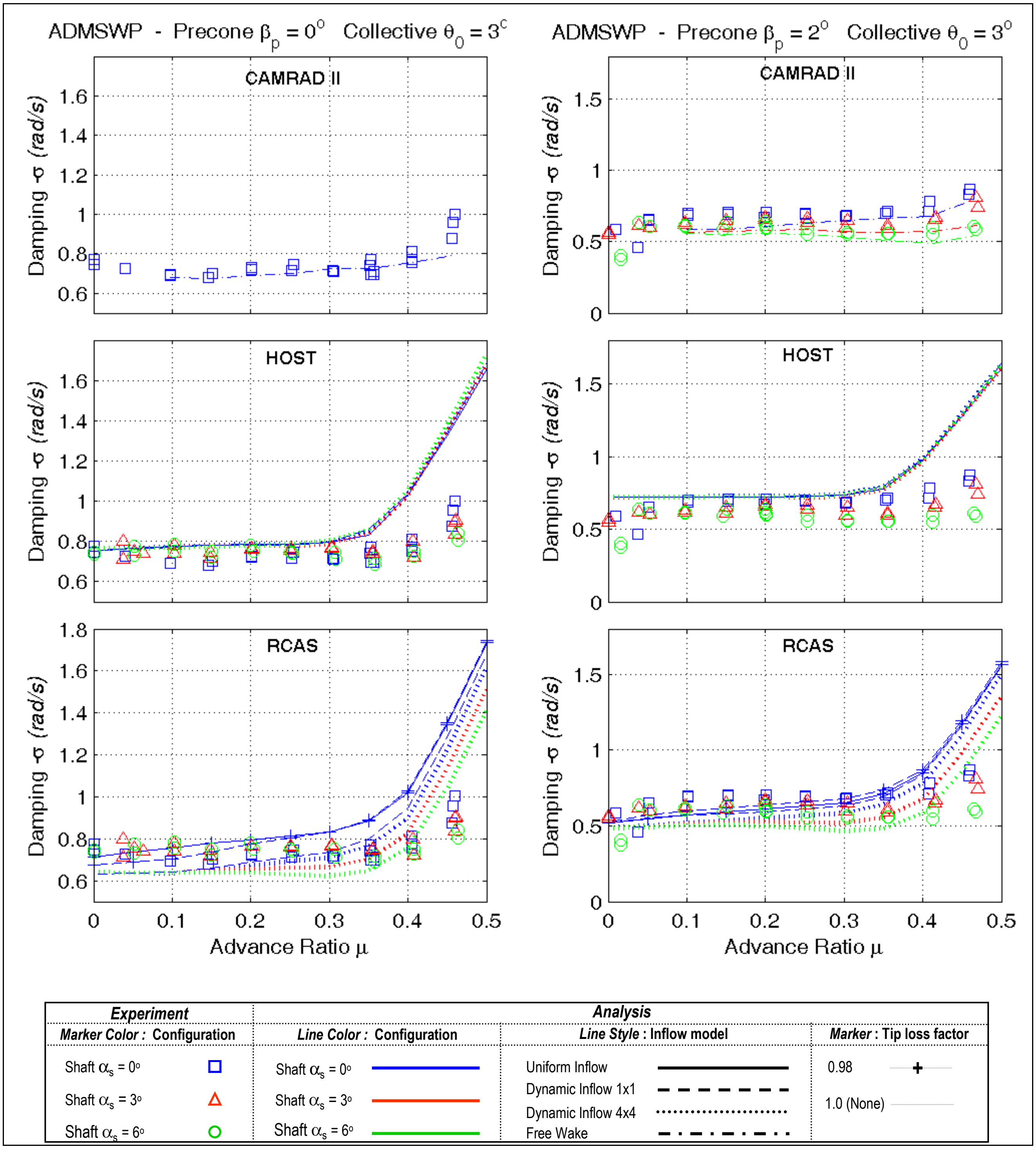

Figure 8: Comparisons for rotors with swept-tip blades in forward flight with shaft angle variations

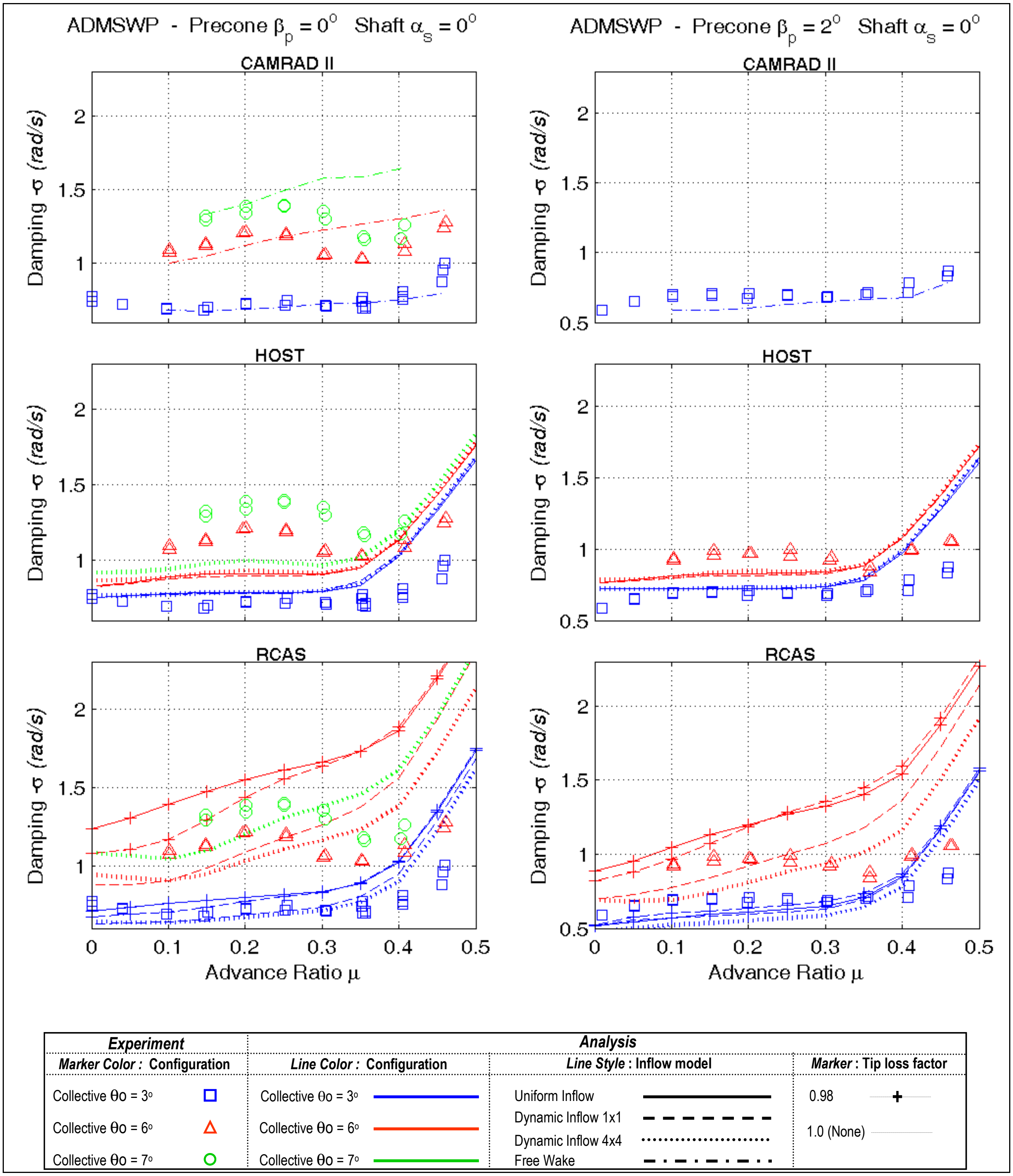

Figure 9: Comparisons for rotors with swept-tip blades in forward flight with collective variations

8. CONCLUSIONS

Experimental data have been compared with results calculated with three comprehensive computer programs CAMRAD II, HOST and RCAS. The experiment measured regressing lag mode damping for two isolated, hingeless, torsionally soft, scaled rotor models in hover and forward flight. The first rotor had straight blades and the second had swept-tip blades. The models were similar, but not identical, and included a variety of inflow models. Based on the comparisons, the following was concluded:

1) There are several basic characteristics of the experiment that provided a qualitative description of the general behavior of the regressing lag mode damping with respect to tip sweep, precone angle, collective pitch angle, shaft angle, and advance ratio. Both the experimental measurements and the results calculated with the three computer programs were consistent with those expectations.
2) For zero precone, the hover results for all programs (ignoring twist irregularities) were symmetric with respect to collective. The experimental data had some asymmetry, only part of which could be explained by twist irregularities in the straight blades. As a result, a model that correlated well with data for positive collectives, correlated poorly for negative collectives, and vice versa.
3) For straight blades, the damping decreased as the order of the dynamic inflow model increased. No such pattern was evident with the swept-tip blades.
4) For straight blades, including tip loss resulted in reduced damping. For swept-tip blades, including tip loss had the opposite effect, increasing damping to levels inconsistent with the measurements. This was consistent with the basic characteristics of the swept-tip and suggested the tip loss model was an over simplification of the aerodynamics of a swept-tip.
5) All of the programs captured the qualitative behavior of the rotor with straight blades, with respect to collective, shaft angle, and advance ratio. However, the quantitative performance was uneven. For instance, all of the programs underestimated the rate of decrease of the damping for $\alpha_S = 6^o$ shaft angle and higher advance ratios at $\theta_0 = 3^o$ collective and $\beta_P = 2^o$ precone. Furthermore, no code identified the exceptionally low damping at $\mu = 0.3$.
6) The most refined inflow models did not always yield the best correlation. No major improvements are evident in hover. In forward flight some improvements are evident at $\beta_P = 2^o$ precone, but there is less evidence at $\beta_P = 0^o$ precone.
7) The damping for a rotor with swept-tip blades exhibits a sinuous up-down-up behavior with respect to advance ratio. Neither CAMRAD II nor RCAS captured this behavior. HOST qualitatively exhibited this behavior to a slight degree, only with the highest order, 4x4, dynamic inflow model. The 1x1 dynamic inflow model produced almost identical results except there was no up-down-up behavior. Quantitatively, the amplitude of the up-down-up behavior was far too small. Both CAMRAD II and RCAS showed an increase in damping with advance ratio that wasn't present in the test data.
8) The rotor with swept-tips exhibits a definite increase in damping at the highest advance ratios. All the codes capture this qualitatively, but quantitatively, CAMRAD II increases are too small and HOST and RCAS increases are much too large.
9) For swept tip blades, the CAMRAD II and RCAS models seemed to be more sensitive to inflow model, shaft angle, or collective than the HOST models.
10) The importance of unsteady aerodynamics was illustrated by a comparison with a quasi-steady case.

ACKNOWLEDGMENTS

The French authors wish to acknowledge the official services of DGA (Délégation Générale pour l'Armement) from the French Ministry of Defence for their support to this cooperation. The US authors are grateful to Dr. Robert.A. Ormiston for sharing his understanding of the experiments and the computer programs.

9. REFERENCES

[1] T.H. Maier, D.L. Sharpe, J. W. Lim, *"Fundamental Investigation of Hingeless Rotor Aeroelastic Stability, Test Data and Correlation"*, American Helicopter Society 51st Annual Forum, Fort Worth, TX, May 9-11, 1995

[2] S. Subramanian, G. Ma, G. H. Gaonkar, T. H. Maier, *"Correlation of Several Aerodynamic Models and Measurements of Hingeless-Rotor Trim and Stability,"* Journal of the American Helicopter Society, Vol. 45, (2), April 2000, pp. 106-117

[3] T.H. Maier, D.L. Sharpe, A.I. Abrego, *"Aeroelastic Stability for Straight and Swept-Tip Rotor Blades in Hover and Forward Flight"*, American Helicopter Society 55th Annual Forum, Montreal, Quebec, Canada May 25-27, 1999

[4] T.H. Maier and A.I. Abrego, *"Analytical Model Sensitivity Study for Aeroelastic Stability of Straight and Swept-Tip Rotor Blades"*, Proceedings of the 26th European Rotorcraft Forum, The Hague, Netherlands, September 2000

[5] A. S. Hopkins and R. A. Ormiston, "*An Examination of Selected Problems in Rotorcraft Aeroelastic Stability*", Proceedings of the American Helicopter Society 60th Annual Forum, Baltimore, Maryland, June 7-10, 2004.

[6] W. Johnson, "*Technology Drivers in the Development of CAMRAD II*", Proceedings of the American Helicopter Society Aeromechanics Specialists Conference, San Francisco, CA, January 19-21, 1994.

[7] W. Johnson, "*CAMRAD II, Comprehensive Analytical Model of Rotorcraft Aerodynamics and Dynamics*", Johnson Aeronautics, Palo Alto, CA, 1992-1997.

[8] A. M. Dequin, B. Benoit (EC), K. Kampa (ECD), W. von Grünhagen (DLR), P. M. Basset, B. Gimonet (ONERA), *"HOST, a General Helicopter Simulation Tool for Germany and France"*, American Helicopter Society 56th Annual Forum, Virginia Beach, Virginia, May 2-4, 2000

[9] P. M. Basset, et al., *"Finite State Rotor Induced Flow Model for Interference and Ground Effect"*, American Helicopter Society 57th Annual Forum, May 2001

[10] H. Saberi, M. Khoshlahjeh, R. A. Ormiston, and M. J. Rutkowski, "*Overview of RCAS and Application to Advanced Rotorcraft Problems*", Proceedings of the American Helicopter Society 44th Decennial Specialist's Conference on Aeromechanics, San Francisco, CA, January 21-23, 2004.

[11] Anon. RCAS User's Manual, Version 2.0, Technical Report USAAMCOM/AFDD TR 02-A-006, US Army Aviation and Missile Command, Moffett Field, CA, June 2003.

[12] Anon. RCAS Theory Manual, Version 2.0, Technical Report USAAMCOM/AFDD TR 02-A-005, US Army Aviation and Missile Command, Moffett Field, CA, June 2003.

[13] A. S. Hopkins and R. A. Ormiston, "*An Examination of Selected Problems in Rotor Blade Structural Mechanics and Dynamics*", Journal of the American Helicopter Society, Vol. 51, (1), January 2006, pp.104-119